



## Cellulases adsorb reversibly on biomass lignin

Djajadi, Demi T.; Pihlajaniemi, Ville; Rahikainen, Jenni; Kruus, Kristiina; Meyer, Anne S.

*Published in:*  
Biotechnology and Bioengineering

*Link to article, DOI:*  
[10.1002/bit.26820](https://doi.org/10.1002/bit.26820)

*Publication date:*  
2018

*Document Version*  
Publisher's PDF, also known as Version of record

[Link back to DTU Orbit](#)

*Citation (APA):*  
Djajadi, D. T., Pihlajaniemi, V., Rahikainen, J., Kruus, K., & Meyer, A. S. (2018). Cellulases adsorb reversibly on biomass lignin. *Biotechnology and Bioengineering*, 115(12), 2869-2880. <https://doi.org/10.1002/bit.26820>

---

### General rights

Copyright and moral rights for the publications made accessible in the public portal are retained by the authors and/or other copyright owners and it is a condition of accessing publications that users recognise and abide by the legal requirements associated with these rights.

- Users may download and print one copy of any publication from the public portal for the purpose of private study or research.
- You may not further distribute the material or use it for any profit-making activity or commercial gain
- You may freely distribute the URL identifying the publication in the public portal

If you believe that this document breaches copyright please contact us providing details, and we will remove access to the work immediately and investigate your claim.

## ARTICLE

## Cellulases adsorb reversibly on biomass lignin

Demi T. Djajadi<sup>1\*</sup> | Ville Pihlajaniemi<sup>2\*</sup> | Jenni Rahikainen<sup>2</sup> | Kristiina Kruus<sup>2</sup> | Anne S. Meyer<sup>1</sup><sup>1</sup>Department of Chemical and Biochemical Engineering, Technical University of Denmark, Kongens Lyngby, Denmark<sup>2</sup>VTT Technical Research Center of Finland Ltd., Finland**Correspondence**Anne S. Meyer, Department of Chemical and Biochemical Engineering, Technical University of Denmark, Søltofts Plads Building 229, Kongens Lyngby 2800, Denmark.  
Email: asme@dtu.dk**Funding information**

BioValue SPIR Innovation Fund Denmark, Grant/Award Number: Case No: 0603-00522B

**Abstract**

Adsorption of cellulases onto lignin is considered a major factor in retarding enzymatic cellulose degradation of lignocellulosic biomass. However, the adsorption mechanisms and kinetics are not well understood for individual types of cellulases. This study examines the binding affinity, kinetics of adsorption, and competition of four monocomponent cellulases of *Trichoderma reesei* during adsorption onto lignin. TrCel7A, TrCel6A, TrCel7B, and TrCel5A were radiolabeled for adsorption experiments on lignin-rich residues (LRRs) isolated from hydrothermally pretreated spruce (L-HPS) and wheat straw (L-HPWS), respectively. On the basis of adsorption isotherms fitted to the Langmuir model, the ranking of binding affinities was TrCel5A > TrCel6A > TrCel7B > TrCel7A on both types of LRRs. The enzymes had a higher affinity to the L-HPS than to the L-HPWS. Adsorption experiments with dilution after 1 and 24 hr and kinetic modeling were performed to quantify any irreversible binding over time. Models with reversible binding parameters fitted well and can explain the results obtained. The adsorption constants obtained from the reversible models agreed with the fitted Langmuir isotherms and suggested that reversible adsorption-desorption existed at equilibrium. Competitive binding experiments showed that individual types of cellulases competed for binding sites on the lignin and the adsorption data fitted the Langmuir adsorption model. Overall, the data strongly indicate that the adsorption of cellulases onto lignin is reversible and the findings have implications for the development of more efficient cellulose degrading enzymes.

**KEYWORDS**

adsorption, biomass, cellulase, competition, lignin, reversible

**1 | INTRODUCTION**

Lignin has been considered as one of the major obstructions in biorefinery operations aiming at enzymatically converting cellulose in lignocellulosic biomass into glucose before further downstream processing (Li, Pu, & Ragauskas, 2016). Nonproductive adsorption of cellulases onto lignin is considered an important mechanism behind

retardation of enzymatic cellulose degradation in lignocellulose-based processes (Liu, Sun, Leu, & Chen, 2016; Saini, Patel, Adsul, & Singhania, 2016; Sipponen et al., 2017). Studies have reported adsorption of cellulases onto lignin isolated from various biomass feedstocks and have correlated such adsorption with the observed retardation of enzymatic degradation of pure model cellulose in the presence of the isolated lignin (Kellock, Rahikainen, Marjamaa, & Kruus, 2017; Rahikainen et al., 2011; Tu, Pan, & Saddler, 2009). Hydrophobic interaction (Sammond et al., 2014; Tu et al., 2009), electrostatic

\*Demi T. Djajadi and Ville Pihlajaniemi have contributed equally to this study.

interaction (Lan, Lou, & Zhu, 2013; Yarbrough et al., 2015), and hydrogen bonding (Sewalt, Glasser, & Beauchemin, 1997; Yu et al., 2014) have been regarded as the cause of the nonproductive binding of cellulases to lignin. However, more recently, it has been recognized that several interactions between the different chemical groups in the lignin and in the enzymes may be occurring simultaneously (Liu et al., 2016; Nakagame, Chandra, Kadla, & Saddler, 2011; Rahikainen, Evans et al., 2013; Sipponen et al., 2017).

Accordingly, several mitigating efforts by including additives such as bovine serum albumin (BSA) and surfactants in the hydrolysis reaction (Börjesson, Engqvist, Sipos, & Tjerneld, 2007; Yang & Wyman, 2006), engineering the charge of the enzymes (Whitehead, Bandi, Berger, Park, & Chundawat, 2017) or changing the pH of the reaction (Lan et al., 2013) have been used with varying degrees of success. However, the precise mechanism in the enzyme–lignin interaction that leads to reduced recoverable activity or cellulose conversion is not well understood, especially with respect to the individual types of enzymes present in a cellulosic mixture. Several studies have indicated irreversible binding and/or reduced recovery of activity during adsorption of cellulases on isolated lignin (Kellock et al., 2017; Rahikainen et al., 2011) or during enzymatic hydrolysis of pretreated lignocellulosic biomass (Gao et al., 2014; Várnai, Viikari, Marjamaa, & Siika-Aho, 2011). Yet, there are also studies reporting that isolated lignin neither retarded the enzymatic cellulose degradation (Barsberg, Selig, & Felby, 2013; Weiss, Börjesson, Pedersen, & Meyer, 2013; Djajadi et al., 2018) nor reduced the recoverable cellulase activity after adsorption (Rodrigues, Leitão, Moreira, Felby, & Gama, 2012). These studies suggested that the binding of the enzymes on lignin is reversible by nature. However, such a phenomenon has not been investigated up to date as the loss of enzyme activity because of nonproductive adsorption onto lignin has in general been considered as irreversible (Saini et al., 2016).

Generally, adsorption of protein onto solid surfaces is known as a dynamic process involving partial exchange of adsorbed and desorbed states. During the process, however, the constant conformational rearrangements between the two states can compromise the structural integrity of the protein, leading to irreversible structural change(s) that can affect subsequent adsorption behavior (Norde, 1986). This denaturation because of protein unfolding has been suggested as the cause of reduced enzymatic cellulose degradation in the presence of lignin (Rahikainen et al., 2011; Sammond et al., 2014), especially at elevated temperature (Börjesson et al., 2007; Rahikainen et al., 2011). Consequently, cellulose hydrolysis by thermostable enzymes was affected less by lignin compared with that performed by enzymes with lesser thermostability (Rahikainen, Moilanen et al., 2013). In this study, well-characterized monocomponent cellulases derived from *Trichoderma reesei* were studied to assess their binding affinity on lignin-rich residues (LRRs) from different biomass feedstocks, to distinguish reversible and irreversible bindings over extended reaction time using kinetic experiments and modeling, as well as to assess their competition with one another during adsorption on lignin.

## 2 | MATERIALS AND METHODS

### 2.1 | Biomass pretreatment and lignin isolation

LRRs were obtained from extensive enzymatic hydrolysis of hydrothermally pretreated spruce (HPS) and wheat straw (HPWS) followed by protease treatment optimized from a previous method (Rahikainen et al., 2011). The hydrothermal pretreatment conditions were 195°C for 15 min ( $\log R_0 = 3.97$ ) for wheat straw (Djajadi et al., 2017) and 200°C for 10 min ( $\log R_0 = 3.94$ ) for spruce. The composition of the LRRs have been determined using the National Renewable Energy Laboratory protocol (Sluiter et al., 2008). The LRRs contained 82.3% and 83.7% total lignin for lignin from HPS (L-HPS) and HPWS (L-HPWS), respectively. The isolation method was shown to remove adsorbed enzymes as indicated by the reduction in nitrogen content of the LRRs (Djajadi et al., 2018; Rahikainen et al., 2011). Even though the isolated LRRs contained residual carbohydrates, the carbohydrates were not accessible to the enzymes and were not traceable to the surface of the LRRs (Djajadi et al., 2018).

### 2.2 | Enzyme purification and characterization

Monocomponent cellulases, that is, cellobiohydrolases (*TrCel7A* and *TrCel6A*) and endoglucanases (EGs: *TrCel7B* and *TrCel5A*) were produced from *Trichoderma reesei* (Teleomorph *Hypocrea jecorina*) at VTT and were purified according to previous work (Suurnäkki et al., 2000). The molecular weights ( $M_{w,s}$ ), isoelectric point (pI), and hydrophobic surface characteristics (patch score) of the enzymes have been determined previously (Kellock et al., 2017; Várnai, Siika-Aho, & Viikari, 2013). The activity of *TrCel7A* and *TrCel6A* was assessed by hydrolyzing 0.1% (w/v) regenerated amorphous cellulose as a substrate using 50 mg/g dosage for 2 hr at 45°C and pH 5.0. The activity of *TrCel7B* and *TrCel5A* was determined using hydroxyethyl cellulose (Sigma-Aldrich Co., MO) 1% (w/v) as a substrate for 2 hr at 45°C and pH 5.0. The products were quantified as reducing sugars using 3,5-dinitrosalicylic acid (Merck, Darmstadt, Germany). Final protein purity and protein concentrations were determined using sodium dodecyl sulfate-polyacrylamide gel electrophoresis analysis (SDS-PAGE) using the Criterion Imaging System (Bio-Rad Laboratories Inc., CA) and the Detergent Compatible (DC) Protein assay (Bio-Rad Laboratories Inc., CA), respectively. The monocomponent enzymes were pure as indicated by the presence of single bands (Supporting Information Figure S1). The details of the enzymes used in this study are presented in Table 1.

### 2.3 | Radiolabeling of the enzymes through reductive methylation

The enzymes (*TrCel7A*, *TrCel6A*, *TrCel7B*, and *TrCel5A*) were radiolabeled with tritium through reductive methylation using tritiated sodium borohydride ( $[^3\text{H}]\text{NaBH}_4$ ) and formaldehyde ( $\text{CH}_2\text{O}$ ) (Means & Feeney, 1968; Tack, Dean, Eilat, Lorenz, & Schechter, 1980) with modifications according to previous works (Rahikainen, Evans et al., 2013; Wahlström, Rahikainen, Kruus, & Suurnäkki, 2014). For the

**TABLE 1** Summary of the characteristics of monocomponent cellulases used in this study

Enzymes	Old name	EC number	Domain architecture	$M_w$ (kDa) <sup>a</sup>	pI <sup>b</sup>	Hydrophobic patch score <sup>b</sup>			Activity <sup>c</sup>
						Core	CBM	Total	
TrCel7A	CBHI	3.2.1.91	GH7-CBM1	56.0	3.6– <u>4.3</u>	6.7	6.6	13.3	5.7%
TrCel6A	CBHII	3.2.1.91	GH6-CBM1	56.7	5.4– <u>6.2</u>	14.1	1.9	16.0	14.8%
TrCel7B	EGI	3.2.1.4	GH7-CBM1	51.9	4.5–4.9, <u>4.7</u>	6.2	0.8	7.0	378.2 nkat/mg
TrCel5A	EGII	3.2.1.4	GH5-CBM1	48.2	<u>5.6</u>	2.6	7.0	9.6	568.4 nkat/mg

Note. CBM: carbohydrate binding module; EC: enzyme commission;  $M_w$ : molecular weight; pI: isoelectric point.

<sup>a</sup>Based on Várnai et al. (2013).

<sup>b</sup>Based on Kellock et al. (2017); major isoform in pI measurement is underlined.

<sup>c</sup>Activity of TrCel7A and TrCel6A is displayed as the degree of regenerated amorphous cellulase hydrolysis, whereas that of TrCel7B and TrCel5A is displayed as a specific activity.

reaction, 3 mg enzyme was buffer exchanged in 0.2 M sodium borate buffer pH 8.5 at 4°C and was incubated on ice. Formaldehyde solution (Sigma-Aldrich Co., MO) was added in fivefold molar excess of the molar concentration of free amino groups in the enzyme. [<sup>3</sup>H]NaBH<sub>4</sub> with 100 mCi activity (5–15 Ci/mmol, PerkinElmer, MA) was dissolved in 0.01 M NaOH (1 Ci/ml) and added to the reaction. After 60 min, the reaction was stopped by transferring the mixture to Econo-Pac 10 DC gel filtration column (Bio-Rad Laboratories Inc., CA) and eluting it with 0.05 M sodium acetate buffer pH 5.0 to exchange the buffer solution. The protein-rich fractions were pooled and transferred to another gel filtration column. The specific radioactivities as determined by liquid scintillation counting (LSC) and protein concentration assay were 0.5, 0.5, 1.7, and 2.8 Ci/mmol for TrCel7A, TrCel6A, TrCel7B, and TrCel5A, respectively. Accordingly, in the subsequent adsorption experiments, the <sup>3</sup>H-labeled enzymes were mixed in 1:20 (for TrCel7A and TrCel6A) and 1:50 dilution ratio (for TrCel7B and TrCel5A) with their nonradiolabeled counterparts to allow accurate detection as done previously (Rahikainen et al., 2013; Wahlström et al., 2014). SDS-PAGE analysis indicated that there was no degradation of the radiolabeled enzymes (Supporting Information Figure S1).

## 2.4 | Adsorption experiments and LSC

All of the enzyme adsorption experiments were performed in 0.05 M sodium acetate buffer pH 5.0 at a substrate concentration of 1% DM (dry matter) and at a temperature of 45°C with moderate mixing. The temperature was chosen because of its relevance to large-scale commercial applications that operate at 37–50°C (Larsen, Haven, & Thirup, 2012). After 1 hr incubation, the experiment was terminated by centrifugation and the supernatant was collected for determination of unbound enzymes using LSC. The supernatant was mixed with Ultima Gold™ XR liquid scintillation cocktail (PerkinElmer, Waltham, MA) and the counts per minute values of the <sup>3</sup>H-labeled enzymes were measured using Tri-Carb 2810 TR LSC (PerkinElmer, Waltham, MA) with 15 min counting time. Enzyme blanks were used to determine the fraction of bound enzyme. Adsorption isotherms were established at the initial protein concentration range of 2–16 μM for L-HPS and 1–8 μM

for L-HPWS in triplicates for each concentration. The adsorption isotherms data were fitted to the one binding-site Langmuir adsorption model:

$$B = B_{\max} \frac{K_{\text{ads}}[F]}{1 + K_{\text{ads}}[F]} \quad (1)$$

where  $B$  is the amount of bound enzyme,  $B_{\max}$  is the maximum adsorption capacity,  $K_{\text{ads}}$  is the Langmuir affinity constant, and  $[F]$  is the concentration of unbound enzyme.

## 2.5 | Reversibility test and kinetic modeling of adsorption

The reversibility test was conducted at similar conditions as with adsorption isotherms. The experiment was performed using TrCel5A and TrCel6A on both L-HPS and L-HPWS. The enzymes were incubated with 1% DM LRRs at concentrations of 4, 8, and 16 μM for L-HPS and 2, 4, and 8 μM for L-HPWS. Subsamples were taken at different time points, centrifuged, and measured to determine the amount of enzyme bound. There were two sets of reactions in which twofold buffer dilution was performed at different time points. In the first set of reaction, the “Early Dilution,” the samples were incubated for 1 hr, after which a subsample was taken and dilution was performed. After dilution, the binding of the enzyme was monitored after 1, 5, and 23 hr by taking subsamples. In the second set of reaction, the “Late Dilution,” the samples were incubated for 24 hr during which subsamples were taken after 1, 6, and 24 hr incubation. After 24 hr, buffer dilution was performed and subsamples were taken after 1, 5, and 23 hr to follow the binding of the enzymes. The experiments were done in duplicates and enzyme blanks were used to determine the amount of the enzyme bound.

Kinetic modeling was performed by using MATLAB R2015a (The Mathworks Inc., MA). The differential equations of a kinetic model were solved by numerical integration using *ode15s* ordinary differential equation solver. The resulting time curves were simultaneously fitted to the combined data from the Early Dilution and Late Dilution experiments of an enzyme–lignin pair by nonlinear regression using *lsqcurvefit*. The fitting parameters included the rate

constants of reversible adsorption  $k_{Rev}$ , desorption  $k_{Des}$ , and irreversible adsorption  $k_{Ir}$  and the maximum adsorption capacity of lignin,  $B_{max}$ . To find the global maximum for the iterative fitting procedure, the fitting was repeated with a full factorial set of initial value combinations with five different initial values (10, 1, 0.01, 0.0001, and 0) for each rate constant and two initial values for the adsorption capacity  $B_{max}$ , including the maximum observed adsorption and its double. For three rate constants and a single  $B_{max}$  this meant 250 repetitions of fitting. The identifiability of the parameters was assessed statistically according to previous work (Pihlajaniemi, Sipponen, Kallioinen, Nyssölä, & Laakso, 2016), by determining the relative standard deviation (RSD) of each parameter from the set of best fitting parameters, including the sets with the  $R^2$  at least 99% of the highest  $R^2$ .

## 2.6 | Competitive binding experiment

Competitive binding experiments were performed similarly as with the adsorption isotherms experiments, except that an equimolar amount of another enzyme type was added on top of the other before the experiments to establish adsorption isotherms. *TrCel5A* and *TrCel6A* were chosen in this experiment, so that in one experiment a radiolabeled *TrCel5A* was accompanied with nonradio-labeled *TrCel6A* and vice versa. The isotherms were established at the ranges of 2–16  $\mu\text{M}$  for L-HPS and 1–8  $\mu\text{M}$  for L-HPWS using triplicates for each concentration. Enzyme blanks were used to determine the fraction of bound enzyme.

## 2.7 | Statistical analysis

One-way analysis of variance was performed using JMP 12 (SAS Institute Inc., NC) with post hoc analysis using the Tukey–Kramer honestly significant difference test at  $p \leq 0.05$ . Fitting of isotherms data to one binding-site Langmuir adsorption model was performed using OriginPro 2016 (OriginLab Corporation, MA).

## 3 | RESULTS AND DISCUSSION

### 3.1 | Binding of monocomponent cellulases on LRRs

Adsorption isotherms of *TrCel7A*, *TrCel6A*, *TrCel7B*, and *TrCel5A* on LRRs isolated from HPS (L-HPS) and wheat straw (L-HPWS) were established to determine their binding affinity in hydrolytic conditions (pH 5.0 and 45°C). The isotherms revealed that *TrCel5A* had the highest affinity on both L-HPS and L-HPWS (Figure 1). In the adsorption on L-HPS, the binding of *TrCel5A* was noticeably higher compared with the other enzymes, although less pronounced in the case of binding on L-HPWS. Visually, the order of the enzymes' affinity was more distinct on L-HPWS compared with L-HPS where the following order of decreasing value can be made: *TrCel5A* > *TrCel6A* > *TrCel7B* > *TrCel7A*. In general, the enzymes had higher

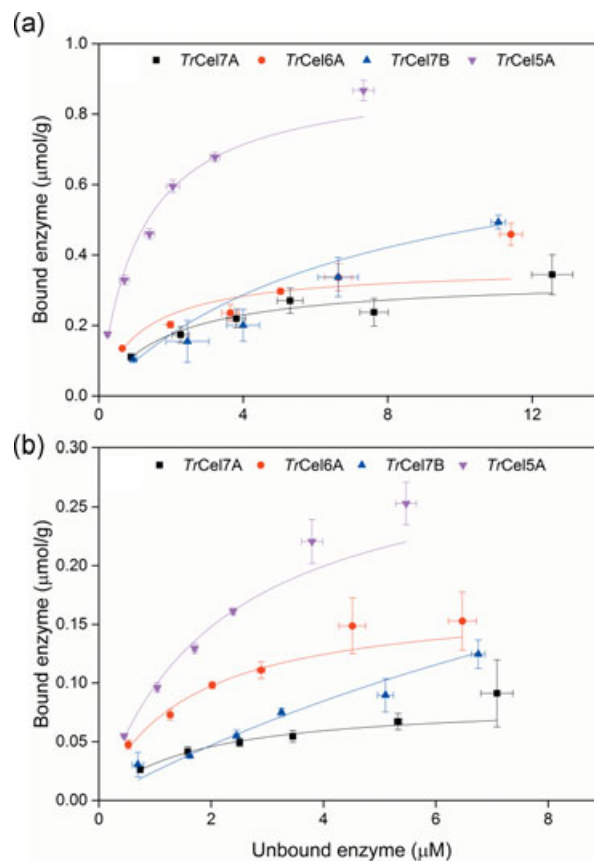


**FIGURE 1** Adsorption isotherms of radiolabeled *TrCel7A*, *TrCel6A*, *TrCel7B*, and *TrCel5A* on lignin-rich residues isolated from hydrothermally pretreated (a) spruce (L-HPS) and (b) wheat straw (L-HPWS) at 45°C, pH 5.0 after 1 hr. Solid lines represent the fitting of the Langmuir adsorption model for one binding-site to the isotherms. Data points and error bars, respectively, represent the average and standard deviation from three experimental replicates [Color figure can be viewed at [wileyonlinelibrary.com](http://wileyonlinelibrary.com)]

affinity on L-HPS compared with L-HPWS as previously shown in the case of radiolabeled *MaCel45A* (*Cel45* EGs from *Melanocarpus albomyces*) (Rahikainen et al., 2013). The labeling procedure has thus been shown to work consistently despite potential modifications to the surface accessible lysine residues. Change in hydrophobicity because of methylation is minimal due to the low number of total lysine residues in the enzymes (6–13 residues). Furthermore, the procedure is known to not affect the positive charge of lysine residues (Tack et al., 1980), making it unlikely for the pI of the protein to be modified as to affect adsorption.

One binding-site Langmuir adsorption model was fitted to the isotherms data to provide quantitative parameters of the binding. The Langmuir adsorption model has previously been used to model the binding of cellulases to lignin (Börjesson et al., 2007; Rahikainen, Evans et al., 2013; Tu et al., 2009) because of its simplicity and versatility despite the inadequacy and shortcomings to depict the adsorption of proteins on solid surface (Latour, 2015; Rabe, Verdes, & Seeger, 2011). The relative association constant ( $\alpha$ ), in particular, has been shown to reflect the relative affinity during the initial slope of the isotherm (Gilkes et al., 1992; Nidetzky, Steiner, Hayn, &

**TABLE 2** Langmuir isotherm parameters from the fitted adsorption data of monocomponent cellulases on isolated lignin-rich residues, L-HPS and L-HPWS, respectively

Adsorbent	Enzyme	$10 \times B_{\max}$ ( $\mu\text{mol/g}$ )	$10 \times K_{\text{ads}}$ ( $\text{L}/\mu\text{mol}$ )	$10 \times \alpha$ ( $\text{L/g}$ )	$R^2$
L-HPS	<i>TrCel7A</i>	$3.34 \pm 0.28$	$5.48 \pm 0.82$	$1.83 \pm 0.31$	0.957
	<i>TrCel6A</i>	$3.66 \pm 0.33$	$8.58 \pm 1.86$	$3.14 \pm 0.74$	0.926
	<i>TrCel7B</i>	$7.94 \pm 1.29$	$1.42 \pm 0.47$	$1.13 \pm 0.42$	0.972
	<i>TrCel5A</i>	$9.13 \pm 0.61$	$8.94 \pm 1.32$	$8.16 \pm 1.32$	0.984
L-HPWS	<i>TrCel7A</i>	$0.84 \pm 0.06$	$6.02 \pm 0.96$	$0.51 \pm 0.09$	0.975
	<i>TrCel6A</i>	$1.72 \pm 0.15$	$6.57 \pm 1.28$	$1.13 \pm 0.24$	0.974
	<i>TrCel7B</i>	$4.27 \pm 1.64$	$0.62 \pm 0.28$	$0.26 \pm 0.16$	0.967
	<i>TrCel5A</i>	$3.07 \pm 0.24$	$4.66 \pm 0.61$	$1.43 \pm 0.22$	0.991

Note.  $B_{\max}$ : maximum adsorption capacity;  $K_{\text{ads}}$ : Langmuir adsorption constant; L-HPS: lignin-rich residues from hydrothermally pretreated spruce; L-HPWS: lignin-rich residues from hydrothermally pretreated wheat straw;  $\alpha$ : relative association constant ( $B_{\max} \times K_{\text{ads}}$ ). The reported constants and errors were obtained from the fitting of three experimental replicates using the one binding-site Langmuir adsorption model.

Claeyssens, 1994; Rahikainen, Evans et al., 2013). Accordingly, the order of affinity based on  $\alpha$  values (Table 2) fits with the visual observation noticed in the isotherms curve for both L-HPS and L-HPWS (Figure 1) and confirmed the previously mentioned ranking of binding affinity:  $TrCel5A > TrCel6A > TrCel7B > TrCel7A$ .

Alternatively, analyzing adsorption at the lower concentration range of an isotherm also provides information on the affinity of the enzyme in nonsaturated conditions. At low initial protein concentration, the ratio of unbound compared to bound enzyme is very low. Therefore the fraction of the bound enzyme reflects the initial affinity toward the substrate without oversaturation of the surface of the adsorbent or excessive interaction among adsorbate molecules. The fraction of bound enzyme at the initial protein concentration of  $2 \mu\text{M}$  after 1 hr showed that *TrCel5A* had the highest binding with 88% and 55% of enzymes adsorbed on both L-HPS and L-HPWS, respectively (Figure 2). The degree of binding

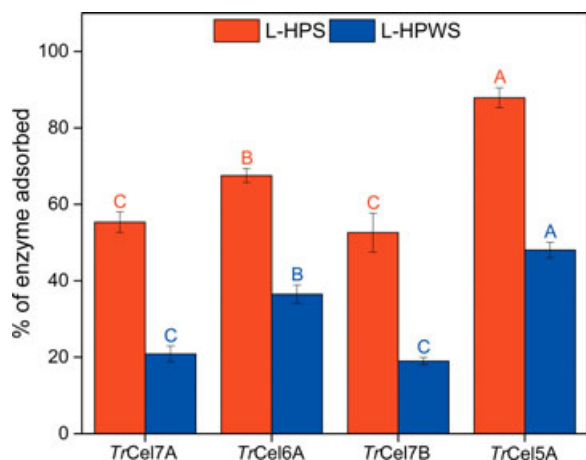


**FIGURE 2** Adsorption of monocomponent cellulases to lignin-rich residues isolated from hydrothermally pretreated spruce (L-HPS) and hydrothermally pretreated wheat straw (L-HPWS) at the initial protein concentration of  $2 \mu\text{M}$  after 1 hr at  $45^\circ\text{C}$ . Different letters indicate significant statistical difference based on ANOVA ( $p \leq 0.05$ ). Data points and error bars, respectively, represent the average and standard deviation from three experimental replicates. ANOVA: analysis of variance [Color figure can be viewed at wileyonlinelibrary.com]

affinity based on the fraction of bound enzyme both on L-HPS and L-HPWS (Figure 2) was:  $TrCel5A > TrCel6A > TrCel7A = TrCel7B$ . To a certain extent, this also confirmed the similar previously established order based on visual observation of the isotherms curve (Figure 1) and fitted  $\alpha$  values (Table 2).

The results in this study evidently showed that *TrCel5A* had the highest binding affinity compared with all the tested enzymes, both in L-HPS and L-HPWS (Figures 1,2). In a recent study, where the same set of enzymes were subjected to binding with model surface lignin isolated from HPS and HPWS on quartz crystal microbalance with dissipation monitoring (QCM-D), *TrCel7B* had the highest binding (Kellock et al., 2017). The finding is in contrast with this study where *TrCel7B* had the second lowest affinity (Table 2). However, based on maximum adsorption capacity ( $B_{\max}$ ), the values of *TrCel7B* and *TrCel5A* were in the same magnitude both in L-HPS and L-HPWS (Table 2), which can explain the discrepancy of the finding in the two works. Nevertheless, a direct comparison between the previous QCM-D work (Kellock et al., 2017) and this current work will be difficult because of different underlying mechanisms in the methods and even properties of the isolated lignin (Rahikainen, Martin-Sampedro et al., 2013). Both current work (Figures 1,2, Table 2) and previous study (Kellock et al., 2017), nevertheless, agreed that *TrCel6A* had the second highest affinity and *TrCel7A* had the lowest affinity from the four tested enzymes.

The binding affinity of the enzymes was compared with their intrinsic properties to find the correlation between the two. *TrCel5A*, which bound the highest, has the lowest molecular weight ( $M_w$ ) of the tested monocomponent cellulases (Table 1). However, the trend is not consistent across the enzymes because *TrCel7A*, which had the lowest affinity, had the second highest  $M_w$ . The highest affinity of *TrCel5A* and *TrCel6A* correlated to their pI values, which are above the experimental pH value of 5.0. This rendered them to be positively charged and therefore increased the tendency to bind to isolated LRRs from HPS and wheat straw, which were previously found to be negatively charged in the experimental pH (Rahikainen, Evans et al., 2013). However, the trend is not consistent because the pI value of the dominant band was lower in *TrCel5A* compared with *TrCel6A*

(Table 1). Estimated hydrophobic patch score did not provide a clear trend either because both the overall and carbohydrate binding module scores were both second highest in the case of *TrCel7A* (Table 1), which had the lowest affinity (Figure 1). At this point, correlating the affinity of the enzymes with their properties was not feasible, yet the enzymes displayed similar ranking of affinity in the two substrates. Experiments at longer duration will be needed to assess the nature of the binding.

### 3.2 | Reversibility test and kinetic modeling of adsorption

Kinetic modeling was applied for studying the proportions and potential mechanisms of reversible and irreversible adsorption of *TrCel6A* and *TrCel5A* on L-HPS and L-HPWS. First, the time course of adsorption and subsequent desorption after dilution of the system by a factor of two were determined. The dilution was performed either after 1 hr (early dilution) or 24 hr of adsorption (late dilution). Three initial enzyme concentrations were used, covering the linear and saturated areas of the adsorption isotherms (Figure 1). The aim was to quantify the proportion of irreversible binding from the difference in desorption after early and late dilution and to provide data for distinguishing the different models. The idea was that the longer incubation before the late dilution would allow irreversible binding to advance further and lead to lower desorption of enzymes compared with the early dilution, which would allow quantification of the proportion and the rate constant of irreversible binding.

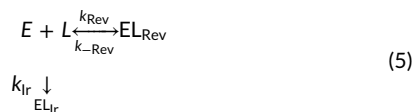
Four different kinetic models were studied. Model 1 (Equation (2)) describes reversible adsorption, which may turn into irreversible by a further first-order reaction, resulting in kinetic Equations (3) and (4), where  $E$  stands for free enzymes,  $L$  for free binding sites, and  $EL$  for bound enzymes, and the subscripts Rev and Ir refer to reversible and irreversible binding, respectively, and the corresponding rate constant  $k$ . The concentration of free sites is the proportion of unoccupied sites multiplied by lignin concentration,  $[L] = (B_{\max} - (EL_{\text{Rev}} + EL_{\text{Ir}})) \cdot [\text{lignin}]$ .



$$\frac{dEL_{\text{Rev}}}{dt} = k_{\text{Rev}}[E][L] - (k_{-\text{Rev}} + k_{\text{Ir}})[EL_{\text{Rev}}] \quad (3)$$

$$\frac{dEL_{\text{Ir}}}{dt} = k_{\text{Ir}}[EL_{\text{Rev}}] \quad (4)$$

Model 2 (Equation (5)) describes separate reversible and irreversible binding on the same binding sites, representing a situation where binding may occur differently, depending on, for example, orientation; therefore, following the Langmuir-kinetics of reversible adsorption (Equation (6)) and a second-order reaction of irreversible binding (Equation (7)) in parallel.



$$\frac{dEL_{\text{Rev}}}{dt} = k_{\text{Rev}}[E][L] - k_{-\text{Rev}}[EL_{\text{Rev}}] \quad (6)$$

$$\frac{dEL_{\text{Ir}}}{dt} = k_{\text{Ir}}[E][L] \quad (7)$$

Models 3 and 4 represent completely reversible (Langmuirian) (Equation (8)) and completely irreversible (Equation (9)) adsorption, each follows the kinetics of Equations (6) and (7), respectively.



The models were fitted to the experimental data and compared in terms of  $R^2$  and parameter identifiability. Identifiability describes whether the parameter value can be determined exclusively, displaying importance (or significance) of the fit, or whether it can adopt an arbitrary value, deeming it irrelevant. The identifiability was described as RSD of each parameter at the optimum fit, determined from the set of repetitions reaching at least 99% of the best fit, according to  $R^2$ .

Majority of adsorption occurred during the first hour, after which only minor changes were observed (Figure 3), indicating that equilibrium was reached within 1 hr of adsorption. *TrCel6A* and *TrCel5A* showed similar adsorption patterns, whereas they differed on L-HPS and L-HPWS (Supporting Information Figures S2–S5). After dilution, minor or no release of enzymes occurred from L-HPS, whereas considerable desorption from L-HPWS-lignin was observed. The lack of desorption from L-HPS appears to suggest irreversible binding, but on a closer look this conclusion turns out to be premature. In fact, completely irreversible adsorption fitted poorly to the data (Supporting Information Figure S6) with  $R^2$  below 0.78 in each case (Table 3). Given the high initial rate of adsorption, the long incubation should have easily allowed completion of irreversible binding, thus leading to either depletion of free enzymes or complete saturation of binding sites. However, such behavior was not observed and instead, equilibrium was reached at each concentration between free and adsorbed enzymes and the endpoints followed a Langmuir isotherm (Supporting Information Figure S6). By definition, both the dynamic equilibrium and Langmuirian behavior indicate reversible adsorption.

Displaying the data from the dilution experiments as binding isotherms revealed that most of the points after dilution either fully or partially returned to the original point before dilution (Supporting Information Figures S7 and S8). In other words, the ascending isotherm (before dilution) overlaps with the descending isotherm (after dilution), displaying no or limited hysteresis in the adsorption. This behavior has also been described as a display of

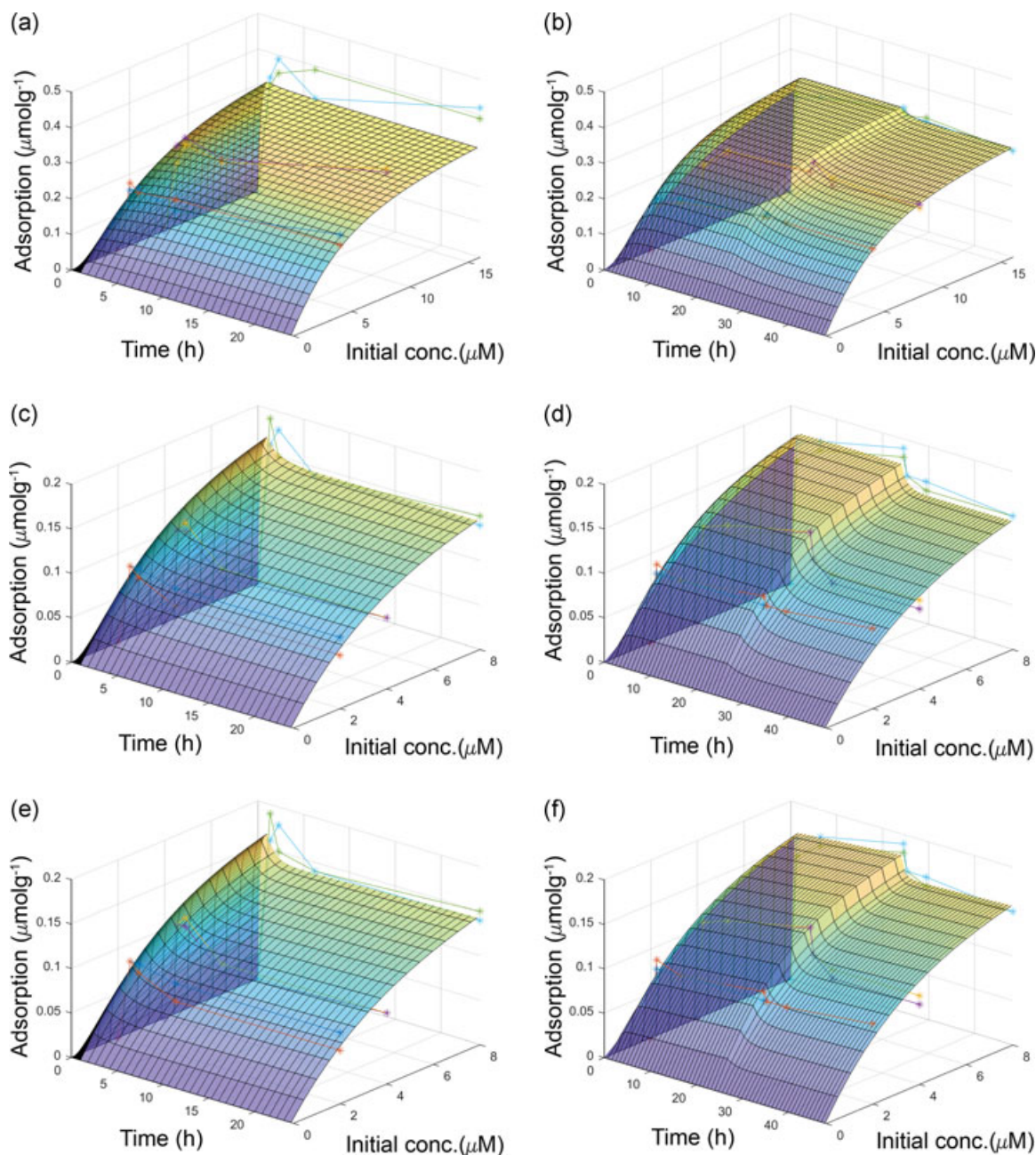


**FIGURE 3** Response surface graphs displaying the fitting of experimental data of *TrCel6A* adsorption on lignin-rich residues isolated from hydrothermally pretreated spruce (L-HPS) (a,b) and hydrothermally pretreated wheat straw (L-HPWS) (c–f) modeled as reversible adsorption (a–d) and using Model 1 (e,f) with early (a,c,e) and late dilution (b,d,f) [Color figure can be viewed at [wileyonlinelibrary.com](http://wileyonlinelibrary.com)]

fully reversible binding during studies on the binding of mono-component cellulases on cellulose (Palonen, Tenkanen, & Linder, 1999; Pellegrini et al., 2014). The Langmuir constants  $K_{ads} = \frac{k_{Rev}}{k_{-Rev}}$  and  $B_{max}$  determined from the kinetic modeling (Table 3) and those determined from the adsorption isotherms data (Table 2) are found to be in agreement with one another (Supporting Information Figure S9). These observations further gave a strong indication of reversible binding on lignin. The adsorption constant ( $K_{ads}$ ) of *TrCel6A* and *TrCel5A* were lower on L-HPWS compared with L-HPS both in the adsorption isotherms fitting (Table 2) and modeling data (Table 3). This indicated lower binding affinity of

cellulases on L-HPWS than L-HPS, which is in accordance with the high desorption on L-HPWS after dilution (Figure 3). The difference in affinity can offer an explanation on the previous observations where L-HPS was found to retard the enzymatic hydrolysis of model cellulose more than L-HPWS (Kellock et al., 2017; Rahikainen, Moilanen et al., 2013).

For L-HPS, the Models 1 and 2 showed a similar fit ( $R^2$  of 0.896–0.923) and parameter values as that of completely reversible adsorption. In contrast, poor identifiability was observed for the irreversible adsorption rate constant  $k_{ir}$  (RSD from 140% to  $4.8 \times 10^{7\%}$ ), indicating that reversible adsorption behavior can fully



**TABLE 3** The values and identifiability of fitting parameters of kinetic modeling

LRRs	Enzyme	Model	Fit $R^2$	Parameters				
				$k_{Rev}$ , $L^2 \cdot (\mu\text{mol} \cdot \text{g} \cdot \text{hr})^{-1}$	$k_{Rev}$ , $L \cdot (\text{g} \cdot \text{hr})^{-1}$	$k_{Ir}^*$	$B_{max}$ ( $\mu\text{mol}/\text{g}$ )	$K_{ads}$ ( $L/\mu\text{mol}$ )
HPS	TrCel6A	Model 1	0.896	0.0157	0.0163	3.82E-10	0.356	0.959
HPS	TrCel6A	Model 2	0.896	0.0120	0.0166	3.64E-03	0.357	0.723
HPS	TrCel6A	Reversible	0.896	0.0157	0.0164		0.356	0.957
HPS	TrCel6A	Irreversible	0.772			0.0217	0.272	
HPS	TrCel5A	Model 1	0.923	0.0165	0.0171	1.45E-07	0.562	0.962
HPS	TrCel5A	Model 2	0.923	0.0154	0.0167	7.81E-04	0.562	0.921
HPS	TrCel5A	Reversible	0.923	0.0160	0.0167		0.562	0.958
HPS	TrCel5A	Irreversible	0.784			0.0158	0.471	
HPWS	TrCel6A	Model 1	0.945	0.0397	0.0855	1.18E-03	0.223	0.464
HPWS	TrCel6A	Model 2	0.936	0.0311	0.0515	3.01E-04	0.217	0.603
HPWS	TrCel6A	Reversible	0.936	0.0314	0.0518		0.217	0.606
HPWS	TrCel6A	Irreversible	0.640			0.0743	0.124	
HPWS	TrCel5A	Model 1	0.967	0.0202	0.0626	4.05E-04	0.385	0.322
HPWS	TrCel5A	Model 2	0.965	0.0140	0.0512	4.49E-03	0.378	0.274
HPWS	TrCel5A	Reversible	0.965	0.0188	0.0525		0.379	0.357
HPWS	TrCel5A	Irreversible	0.570			0.0332	0.170	
Identifiability (RSD at optimum fit)								
LRRs	Enzyme	Model	Fit $R^2$	$k_{Rev}$	$k_{Rev}$	$k_{Ir}$	$B_{max}$	
HPS	TrCel6A	Model 1	0.896	9%	9%	4.86E+07%	3%	
HPS	TrCel6A	Model 2	0.896	46%	10%	140%	3%	
HPS	TrCel6A	Reversible	0.896	4%	10%		3%	
HPS	TrCel6A	Irreversible	0.772			9%	1%	
HPS	TrCel5A	Model 1	0.923	19%	23%	2.35E+05%	4%	
HPS	TrCel5A	Model 2	0.923	28%	11%	513%	4%	
HPS	TrCel5A	Reversible	0.923	10%	10%		5%	
HPS	TrCel5A	Irreversible	0.784			0%	0%	
HPWS	TrCel6A	Model 1	0.945	71%	65%	9%	4%	
HPWS	TrCel6A	Model 2	0.936	30%	8%	3.03E+03%	3%	
HPWS	TrCel6A	Reversible	0.936	3%	10%		4%	
HPWS	TrCel6A	Irreversible	0.640			31%	3%	
HPWS	TrCel5A	Model 1	0.967	78%	71%	49%	10%	
HPWS	TrCel5A	Model 2	0.965	55%	10%	159%	13%	
HPWS	TrCel5A	Reversible	0.965	25%	8%		13%	
HPWS	TrCel5A	Irreversible	0.570			0%	0%	

Note. HPS: hydrothermally pretreated spruce; HPWS: hydrothermally pretreated wheat straw; RSD: relative standard deviation.

\* $k_{Ir}$  is a first-order rate constant with the unit  $L \cdot (\text{g} \cdot \text{hr})^{-1}$  in Model 1 and a second-order rate constant with the unit  $L^2 \cdot (\mu\text{mol} \cdot \text{g} \cdot \text{hr})^{-1}$  in other models.

explain the results. No quantifiable irreversible binding was observed and the reason for low desorption was high affinity of L-HPS (Table 3). For L-HPWS, a higher amount of desorption provided a higher resolution for determining irreversible binding. Model 1 showed a slightly better fit for both enzymes ( $R^2$  of 0.945 and 0.967) compared with reversible binding (0.936 and 0.965) with a relevant

irreversible binding rate (RSD of  $k_{Ir}$  lower than that of  $k_{Rev}$  and  $k_{Rev}$ ), whereas Model 2 neither provided improvement in fit nor relevance of  $k_{Ir}$  (Table 3). This suggested the possibility of partial irreversible binding on L-HPWS, that is, the enzymes are first bound reversibly, which is then followed by further interactions leading to irreversible binding. This is in line with the idea of protein unfolding taking place

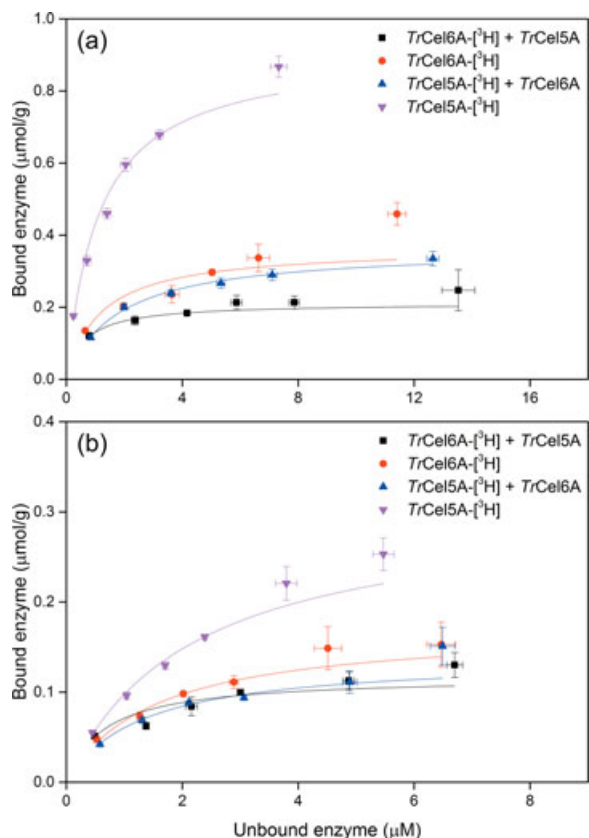


**FIGURE 4** Competitive binding isotherms of *TrCel6A* and *TrCel5A* on lignin-rich residues isolated from hydrothermally pretreated (a) spruce (L-HPS) and (b) wheat straw (L-HPWS) at 45°C, pH 5.0 after 1 hr. The tritium symbol ( $^3\text{H}$ ) indicates radiolabeled enzyme. Solid lines represent the fitting of the Langmuir adsorption model for one binding-site to the isotherms. Data points and error bars, respectively, represent the average and standard deviation from three experimental replicates [Color figure can be viewed at [wileyonlinelibrary.com](http://wileyonlinelibrary.com)]

after binding on lignin (Rahikainen et al., 2011; Rahikainen, Moilanen et al., 2013; Sammond et al., 2014).

The overall good fitting ( $R^2 \approx 0.9$ ) of the Models 1–3 nevertheless pointed out that the adsorption of monocomponent cellulases on lignin

is reversible by nature, instead of being fully irreversible. The good identifiability of reversible adsorption constants, especially in Model 3 where they were better than that in Models 1 and 2, implied that the completely reversible adsorption model alone can explain the findings. Although in some ways the statement might seem contradictory to the previous understanding, this finding illustrates the need for a redefinition of the term irreversibility and highlights that reversibility of adsorption should not be confused with binding affinity. Distinguishing between the two can be complicated, therefore, for practical purposes the activity of the enzyme during binding onto lignin should also be investigated. Loss of activity can correlate to irreversible binding, even though that does not necessarily denote a direct causal relationship. Hence this points to the need to understand the precise mechanism leading to the loss of enzyme activity. Good fitting of Model 1 in this work confirmed and expanded the nuances of the explanation of previous findings (Rahikainen et al., 2011). Initially, the enzymes constantly change structural conformation as they adsorb and desorb reversibly. Incubation at elevated temperature increases the rate of the process and thus the binding affinity. As the process continues, eventually the protein structure unfolds and renders the enzymes to be bound irreversibly at a certain extent, losing activity. In future work, it would be relevant to assess whether the loss of enzyme activity is aggravated at high substrate concentration (10%–30% DM) because of an increased rate of adsorption, and/or whether the binding kinetics may be affected. It remains to be seen by future work whether the loss of enzyme activity and the change to irreversible binding on lignin occur sequentially, separately or simultaneously. Finally, it is important to stress that while the binding is reversible, the loss of activity because of denaturation is irreversible.

### 3.3 | Competitive binding of cellulases

Competitive binding study was performed to find if there is competition between selected monocomponent cellulases *TrCel6A* and *TrCel5A*, which had the highest binding affinity based on the adsorption isotherms (Figures 1 and 2, Table 2). In this experimental

**TABLE 4** Langmuir isotherm parameters from the fitted adsorption data of competitive binding of *TrCel6A* and *TrCel5A* on isolated lignin-rich residues

Adsorbent	Enzyme	$10 \times B_{\max}$ ( $\mu\text{mol/g}$ )	$10 \times K_{\text{ads}}$ ( $\text{L}/\mu\text{mol}$ )	$10 \times \alpha$ ( $\text{L/g}$ )	$R^2$
L-HPS	<i>TrCel6A</i> - $^3\text{H}$	$3.66 \pm 0.33$	$8.58 \pm 1.86$	$3.14 \pm 0.74$	0.926
	<i>TrCel6A</i> - $^3\text{H}$ + <i>TrCel5A</i>	$2.11 \pm 0.05$	$16.3 \pm 2.87$	$3.43 \pm 0.61$	0.948
	<i>TrCel5A</i> - $^3\text{H}$	$9.13 \pm 0.61$	$8.94 \pm 1.32$	$8.16 \pm 1.32$	0.984
	<i>TrCel5A</i> - $^3\text{H}$ + <i>TrCel6A</i>	$3.64 \pm 0.12$	$5.66 \pm 0.45$	$2.06 \pm 0.18$	0.992
L-HPWS	<i>TrCel6A</i> - $^3\text{H}$	$1.72 \pm 0.15$	$6.57 \pm 1.28$	$1.13 \pm 0.24$	0.974
	<i>TrCel6A</i> - $^3\text{H}$ + <i>TrCel5A</i>	$1.17 \pm 0.11$	$15.4 \pm 3.17$	$1.80 \pm 0.41$	0.898
	<i>TrCel5A</i> - $^3\text{H}$	$3.07 \pm 0.24$	$4.66 \pm 0.61$	$1.43 \pm 0.22$	0.991
	<i>TrCel5A</i> - $^3\text{H}$ + <i>TrCel6A</i>	$1.38 \pm 0.09$	$7.79 \pm 1.29$	$1.08 \pm 0.19$	0.979

Note.  $B_{\max}$ : maximum adsorption capacity;  $K_{\text{ads}}$ : Langmuir adsorption constant; L-HPS: lignin-rich residues from hydrothermally pretreated spruce; L-HPWS: lignin-rich residues from hydrothermally pretreated wheat straw;  $\alpha$ : relative association constant ( $B_{\max} \times K_{\text{ads}}$ ). The reported constants and errors were obtained from fitting of three experimental replicates using one binding-site Langmuir adsorption model.

setup, only the binding of the radiolabeled enzyme was recorded. In the equimolar presence of one another, the enzymes showed competitive binding in the isotherms (Figure 4). The presence of TrCel6A reduced the binding of labeled TrCel5A significantly, whereas the presence of TrCel5A had a less pronounced effect on the binding of labeled TrCel6A. The reduction of the binding was clearly visible in both L-HPS (Figure 4a) and L-HPWS (Figure 4b).

Fitting of one binding-site Langmuir adsorption model to the competitive adsorption isotherms still showed good fit in general (Table 4). The maximum adsorption capacity ( $B_{\max}$ ) of TrCel6A was less affected by TrCel5A, whereas the  $B_{\max}$  of TrCel5A was reduced more significantly by TrCel6A both in L-HPS and L-HPWS (Table 4). The  $B_{\max}$  values of the mixture constituted by the two enzymes were nevertheless almost similar in magnitude (Table 4). This indicated that both enzymes competed for similar binding sites and TrCel6A predominated the competitive binding albeit lower  $B_{\max}$  value. Previously it was suggested that the Vroman effect was present in a cellulolytic enzyme mixture where enzymes of greater affinity displaced others of lesser affinity (Yarbrough et al., 2015). In this study, affinity did not seem to be the factor because TrCel5A had higher, if not similar, affinity to TrCel6A based on both  $\alpha$  and  $K_{\text{ads}}$  (Table 4). However, in the original study that coined the Vroman effect, it was shown that proteins with larger size ( $M_w$ ) displaced the smaller ones (Vroman & Adams, 1969). Accordingly, TrCel6A is indeed larger than TrCel5A (Table 1), therefore suggesting size as a plausible factor that governs competitive binding.

The presence of competitive binding between two enzymes showed that monitoring the adsorption of a multicomponent system, such as cellulases, can be difficult to perform. Nevertheless, the presence of competition and good fitting to the Langmuir model also suggest that the binding of cellulases on lignin is exchangeable and thus reversible by nature. The finding thus supports the previous observations in this work and points that the binding of cellulases on lignin is both reversible and competitive as in the case of the binding of cellulases on cellulose (Kyriacou, Neufeld, & MacKenzie, 1989; Pellegrini et al., 2014).

## 4 | CONCLUSIONS

The present work indicates that despite differences in the binding affinity of individual monocomponent cellulases, the binding is reversible by nature. Modeling of kinetic experiments suggests the possibility of previously reversible binding turning to irreversible which can explain the previous observations on retardation of enzymatic cellulose conversion in the presence of lignin. Because of the reversible nature of binding, the negative effect of lignin can plausibly be alleviated by including additives in the reaction. Given the indication that the binding turns irreversible hence losing activity because of structural unfolding over time at elevated temperature, engineering or finding novel enzymes with improved thermostability can be an avenue to pursue. Future studies should be directed into deciphering the underlying mechanism and factors that govern the deactivation of the enzyme by lignin, especially at high substrate concentration. The competition among cellulases in the

adsorption on lignin highlights the necessity to develop methods able to distinguish the binding and activity of individual enzymes in a mixture to identify and selectively improve the necessary enzyme component.

## ACKNOWLEDGMENTS

D.T.D. is funded by the BioValue SPIR, Strategic Platform for Innovation and Research on value-added products from biomass, which is cofunded by The Innovation Fund Denmark, Case No: 0603-00522B. Miriam Kellock is thanked for preparing the L-HPS.

## CONFLICTS OF INTEREST

The authors declare that they have no conflicts of interest.

## NOMENCLATURE

$B_{\max}$	maximum adsorption constant ( $\mu\text{mol/g}$ )
$E$	free enzymes ( $\mu\text{mol/L}$ )
$EL$	bound enzymes ( $\mu\text{mol/g}$ )
$L$	free binding sites in lignin-rich residues ( $\text{g/L}$ )
$K_{\text{ads}}$	Langmuir adsorption constant ( $\text{L}/\mu\text{mol}$ )
$k_{\text{Ir}}$	irreversible adsorption constant ( $\text{L}\cdot(\text{g}\cdot\text{hr})^{-1}$ in Model 1; otherwise $\text{L}^2\cdot(\mu\text{mol}\cdot\text{g}\cdot\text{hr})^{-1}$ in other models)
$k_{\text{Rev}}$	reversible adsorption constant ( $\text{L}^2\cdot(\mu\text{mol}\cdot\text{g}\cdot\text{hr})^{-1}$ )
$k_{\text{Rev}}$	reversible desorption constant ( $\text{L}\cdot(\text{g}\cdot\text{h})^{-1}$ )
$\alpha$	relative association constant ( $\text{L/g}$ )

## ORCID

Demi T. Djajadi  <http://orcid.org/0000-0002-4131-3228>

Ville Pihlajaniemi  <http://orcid.org/0000-0002-8220-6656>

Jenni Rahikainen  <http://orcid.org/0000-0002-4646-6522>

Kristiina Kruus  <http://orcid.org/0000-0003-4749-264X>

Anne S. Meyer  <http://orcid.org/0000-0001-8910-9931>

## REFERENCES

- Barsberg, S., Selig, M. J., & Felby, C. (2013). Impact of lignins isolated from pretreated lignocelluloses on enzymatic cellulose saccharification. *Biotechnology Letters*, 35(2), 189–195. <https://doi.org/10.1007/s10529-012-1061-x>
- Börjesson, J., Engqvist, M., Sipos, B., & Tjerneld, F. (2007). Effect of poly (ethylene glycol) on enzymatic hydrolysis and adsorption of cellulase enzymes to pretreated lignocellulose. *Enzyme and Microbial Technology*, 41(1–2), 186–195. <https://doi.org/10.1016/j.enzmictec.2007.01.003>
- Djajadi, D. T., Hansen, A. R., Jensen, A., Thygesen, L. G., Pinelo, M., Meyer, A. S., & Jørgensen, H. (2017). Surface properties correlate to the digestibility of hydrothermally pretreated lignocellulosic poaceae biomass feedstocks. *Biotechnology for Biofuels*, 10(1), 49. <https://doi.org/10.1186/s13068-017-0730-3>
- Djajadi, D. T., Jensen, M. M., Oliveira, M., Jensen, A., Thygesen, L. G., Pinelo, M., ... Meyer, A. S. (2018). Lignin from hydrothermally pretreated grass biomass retards enzymatic cellulose degradation

- by acting as a physical barrier rather than by inducing nonproductive adsorption of enzymes. *Biotechnology for Biofuels*, 11(1), 85. <https://doi.org/10.1186/s13068-018-1085-0>
- Gao, D., Haarmeyer, C., Balan, V., Whitehead, T. a, Dale, B. E., & Chundawat, S. P. (2014). Lignin triggers irreversible cellulase loss during pretreated lignocellulosic biomass saccharification. *Biotechnology for Biofuels*, 7(1), 175. <https://doi.org/10.1186/s13068-014-0175-x>
- Gilkes, N. R., Jervis, E., Henriessat, B., Tekant, B., Miller RC, Jr, Warren, R. A., & Kilburn, D. G. (1992). The adsorption of a bacterial cellulase and its two isolated domains to crystalline cellulose. *Journal of Biological Chemistry*, 267(10), 6743–6749.
- Kellock, M., Rahikainen, J., Marjamaa, K., & Kruus, K. (2017). Lignin-derived inhibition of monocomponent cellulases and a xylanase in the hydrolysis of lignocellulosics. *Bioresource Technology*, 232, 183–191. <https://doi.org/10.1016/j.biortech.2017.01.072>
- Kyriacou, A., Neufeld, R. J., & MacKenzie, C. R. (1989). Reversibility and competition in the adsorption of *Trichoderma reesei* cellulase components. *Biotechnology and Bioengineering*, 33(5), 631–637. <https://doi.org/10.1002/bit.260330517>
- Lan, T. Q., Lou, H., & Zhu, J. Y. (2013). Enzymatic saccharification of lignocelluloses should be conducted at elevated pH 5.2–6.2. *Bioenergy Research*, 6, 476–485. <https://doi.org/10.1007/s12155-012-9273-4>
- Larsen, J., Haven, M. Ø., & Thirup, L. (2012). Inbicon makes lignocellulosic ethanol a commercial reality. *Biomass & Bioenergy*, 46, 36–45. <https://doi.org/10.1016/j.biombioe.2012.03.033>
- Latour, R. A. (2015). The Langmuir isotherm: A commonly applied but misleading approach for the analysis of protein adsorption behavior. *Journal of Biomedical Materials Research - Part A*, 103(3), 949–958. <https://doi.org/10.1002/jbm.a.35235>
- Li, M., Pu, Y., & Ragauskas, A. J. (2016). Current understanding of the correlation of lignin structure with biomass recalcitrance. *Frontiers in Chemistry*, 4, 45. <https://doi.org/10.3389/fchem.2016.00045>
- Liu, H., Sun, J., Leu, S.-Y., & Chen, S. (2016). Toward a fundamental understanding of cellulase-lignin interactions in the whole slurry enzymatic saccharification process. *Biofuels, Bioproducts and Biorefining*, 10, 648–663. <https://doi.org/10.1002/bbb>
- Means, G. E., & Feeney, R. E. (1968). Reductive alkylation of amino groups in proteins. *Biochemistry*, 7(1965), 2192–2201. <https://doi.org/10.1021/bi00846a023>
- Nakagame, S., Chandra, R. P., Kadla, J. F., & Saddler, J. N. (2011). The isolation, characterization and effect of lignin isolated from steam pretreated Douglas-fir on the enzymatic hydrolysis of cellulose. *Bioresource Technology*, 102(6), 4507–4517. <https://doi.org/10.1016/j.biortech.2010.12.082>
- Nidetzky, B., Steiner, W., Hayn, M., & Claeysens, M. (1994). Cellulose hydrolysis by the cellulases from *Trichoderma reesei*: A new model for synergistic interaction. *The Biochemical Journal*, 298(1994), 705–710.
- Norde, W. (1986). Adsorption of proteins from solution at the solid-liquid interface. *Advances in Colloid and Interface Science*, 25(C), 267–340. [https://doi.org/10.1016/0001-8686\(86\)80012-4](https://doi.org/10.1016/0001-8686(86)80012-4)
- Palonen, H., Tenkanen, M., & Linder, M. (1999). Dynamic interaction of *Trichoderma reesei* cellobiohydrolases Cel6A and Cel7A and cellulose at equilibrium and during hydrolysis. *Applied and Environmental Microbiology*, 65(12), 5229–5233.
- Pellegrini, V. O. A., Lei, N., Kyasaram, M., Olsen, J. P., Badino, S. F., Windahl, M. S., ... Westh, P. (2014). Reversibility of substrate adsorption for the cellulases Cel7A, Cel6A, and Cel7B from *Hypocrea jecorina*. *Langmuir*, 30(42), 12602–12609. <https://doi.org/10.1021/la5024423>
- Pihlajaniemi, V., Sipponen, M. H., Kallioinen, A., Nyyssölä, A., & Laakso, S. (2016). Rate-constraining changes in surface properties, porosity and hydrolysis kinetics of lignocellulose in the course of enzymatic saccharification. *Biotechnology for Biofuels*, 9(1), 18. <https://doi.org/10.1186/s13068-016-0431-3>
- Rabe, M., Verdes, D., & Seeger, S. (2011). Understanding protein adsorption phenomena at solid surfaces. *Advances in Colloid and Interface Science*, 162(1–2), 87–106. <https://doi.org/10.1016/j.cis.2010.12.007>
- Rahikainen, J., Mikander, S., Marjamaa, K., Tamminen, T., Lappas, A., Viikari, L., & Kruus, K. (2011). Inhibition of enzymatic hydrolysis by residual lignins from softwood—Study of enzyme binding and inactivation on lignin-rich surface. *Biotechnology and Bioengineering*, 108(12), 2823–2834. <https://doi.org/10.1002/bit.23242>
- Rahikainen, J. L., Evans, J. D., Mikander, S., Kallioinen, A., Puranen, T., Tamminen, T., ... Kruus, K. (2013). Cellulase-lignin interactions—The role of carbohydrate-binding module and pH in non-productive binding. *Enzyme and Microbial Technology*, 53(5), 315–321. <https://doi.org/10.1016/j.enzmictec.2013.07.003>
- Rahikainen, J., Martin-Sampedro, R., Heikkinen, H., Rovio, S., Marjamaa, K., Tamminen, T., ... Kruus, K. (2013). Inhibitory effect of lignin during cellulose bioconversion: The effect of lignin chemistry on non-productive enzyme adsorption. *Bioresource Technology*, 133, 270–278. <https://doi.org/10.1016/j.biortech.2013.01.075>
- Rahikainen, J. L., Moilanen, U., Nurmi-Rantala, S., Lappas, A., Koivula, A., Viikari, L., & Kruus, K. (2013). Effect of temperature on lignin-derived inhibition studied with three structurally different cellobiohydrolases. *Bioresource Technology*, 146, 118–125. <https://doi.org/10.1016/j.biortech.2013.07.069>
- Rodrigues, A. C., Leitão, A. F., Moreira, S., Felby, C., & Gama, M. (2012). Recycling of cellulases in lignocellulosic hydrolysates using alkaline elution. *Bioresource Technology*, 110, 526–533. <https://doi.org/10.1016/j.biortech.2012.01.140>
- Saini, J. K., Patel, A. K., Adsul, M., & Singhania, R. R. (2016). Cellulase adsorption on lignin: A roadblock for economic hydrolysis of biomass. *Renewable Energy*, 98, 29–42. <https://doi.org/10.1016/j.renene.2016.03.089>
- Sammond, D. W., Yarbrough, J. M., Mansfield, E., Bomble, Y. J., Hobdley, S. E., Decker, S. R., ... Crowley, M. F. (2014). Predicting enzyme adsorption to lignin films by calculating enzyme surface hydrophobicity. *Journal of Biological Chemistry*, 289(30), 20960–20969. <https://doi.org/10.1074/jbc.M114.573642>
- Sewalt, V. J. H., Glasser, W. G., & Beauchemin, K. A. (1997). Lignin impact on fiber degradation . 3. Reversal of inhibition of enzymatic hydrolysis by chemical modification of lignin and by additives. *Journal of Agricultural and Food Chemistry*, 45, 1823–1828 <https://doi.org/10.1021/jf9608074>
- Sipponen, M. H., Rahikainen, J., Leskinen, T., Pihlajaniemi, V., Mattinen, M. -L., Lange, H., ... Österberg, M. (2017). Structural changes of lignin in biorefinery pretreatments and consequences to enzyme-lignin interactions—Open access. *Nordic Pulp and Paper Research Journal*, 32(4), 550–571. <https://doi.org/10.3183/NPPRJ-2017-32-04-p550-571>
- Sluiter, A., Hames, B., Ruiz, R., Scarlata, C., Sluiter, J., Templeton, D., & Crocker, D. (2008). *Determination of structural carbohydrates and lignin in biomass*. (Report No. NREL/TP-510-42618). Golden, CO: Laboratory Analytical Procedure (LAP).
- Suurnäkki, A., Tenkanen, M., Siika-Aho, M., Niku-Paavola, M. L., Viikari, L., & Buchert, J. (2000). *Trichoderma reesei* cellulases and their core domains in the hydrolysis and modification of chemical pulp. *Cellulose*, 7(2), 189–209. <https://doi.org/10.1023/A:1009280109519>
- Tack, B. F., Dean, J., Eilat, D., Lorenz, P. E., & Schechter, A. N. (1980). Tritium labeling of proteins to high specific radioactivity by reductive methylation. *Journal of Biological Chemistry*, 255(18), 8842–8847.
- Tu, M., Pan, X., & Saddler, J. N. (2009). Adsorption of cellulase on cellulosic enzyme lignin from lodgepole pine. *Journal of Agricultural and Food Chemistry*, 57(17), 7771–7778. <https://doi.org/10.1021/jf901031m>
- Vroman, L., & Adams, A. L. (1969). Findings with the recording ellipsometer suggesting rapid exchange of specific plasma proteins at liquid/solid interfaces. *Surface Science*, 16, 438–446. [https://doi.org/10.1016/0039-6028\(69\)90037-5](https://doi.org/10.1016/0039-6028(69)90037-5)
- Várnai, A., Siika-Aho, M., & Viikari, L. (2013). Carbohydrate-binding modules (CBMs) revisited: Reduced amount of water counterbalances

- the need for CBMs. *Biotechnology for Biofuels*, 6, 30. <https://doi.org/10.1186/1754-6834-6-30>
- Várnai, A., Viikari, L., Marjamaa, K., & Siika-Aho, M. (2011). Adsorption of monocomponent enzymes in enzyme mixture analyzed quantitatively during hydrolysis of lignocellulose substrates. *Bioresource Technology*, 102(2), 1220–1227. <https://doi.org/10.1016/j.biortech.2010.07.120>
- Wahlström, R., Rahikainen, J., Kruus, K., & Suurnäkki, A. (2014). Cellulose hydrolysis and binding with *Trichoderma reesei* Cel5A and Cel7A and their core domains in ionic liquid solutions. *Biotechnology and Bioengineering*, 111(4), 726–733. <https://doi.org/10.1002/bit.25144>
- Weiss, N., Börjesson, J., Pedersen, L. P., & Meyer, A. S. (2013). Enzymatic lignocellulose hydrolysis: Improved cellulase productivity by insoluble solids recycling. *Biotechnology for Biofuels*, 6, 5. <https://doi.org/10.1186/1754-6834-6-5>
- Whitehead, T. A., Bandi, C. K., Berger, M., Park, J., & Chundawat, S. P. S. (2017). Negatively supercharging cellulases render them lignin-resistant. *ACS Sustainable Chemistry and Engineering*, 5(7), 6247–6252. <https://doi.org/10.1021/acssuschemeng.7b01202>
- Yang, B., & Wyman, C. E. (2006). BSA treatment to enhance enzymatic hydrolysis of cellulose in lignin containing substrates. *Biotechnology and Bioengineering*, 94(5), 611–617. <https://doi.org/10.1002/bit>
- Yarbrough, J. M., Mittal, A., Mansfield, E., Taylor, L. E., Hobdey, S. E., Sammond, D. W., ... Vinzant, T. B. (2015). New perspective on glycoside hydrolase binding to lignin from pretreated corn stover. *Biotechnology for Biofuels*, 8(1), 214. <https://doi.org/10.1186/s13068-015-0397-6>
- Yu, Z., Gwak, K.-S., Treasure, T., Jameel, H., Chang, H., & Park, S. (2014). Effect of lignin chemistry on the enzymatic hydrolysis of woody biomass. *ChemSusChem*, 7, 1942–1950. <https://doi.org/10.1002/cssc.201400042>

## SUPPORTING INFORMATION

Additional supporting information may be found online in the Supporting Information section at the end of the article.

**How to cite this article:** Djajadi DT, Pihlajaniemi V, Rahikainen J, Kruus K, Meyer AS. Cellulases adsorb reversibly on biomass lignin. *Biotechnology and Bioengineering*. 2018;115:2869–2880. <https://doi.org/10.1002/bit.26820>